Stability and Liftoff of a N_2-in-H_2 Jet Flame in a Vitiated Co-flow at Atmospheric Pressure

A. North[1*], D. Frederick[1], J.-Y. Chen[1], R. Dibble[1], and A. Gruber[2]

[1]50B Hesse Hall, Department of Mechanical Engineering, University of California Berkeley,
Berkeley, CA 94720-1740, USA
[2]SINTEF Energy Research, 7465 Trondheim, Norway

Abstract

The stability and liftoff characteristics of a nitrogen (N_2) diluted hydrogen (H_2) jet flame in a vitiated co-flow are investigated experimentally with particular attention focused on regimes where multiple stabilization mechanisms are active. Information gleaned from this research is instrumental for informing modeling approaches in flame transition situations when both autoignition and flame propagation influence combustion characteristics. Stability regime diagrams which outline the conditions under which the flame is attached, lifted, blown-out, and unsteady are experimentally developed and explored. The lifted regime is further characterized in determining liftoff height dependence on N_2 dilution, jet velocity, and co-flow equivalence ratio (or essentially, co-flow temperature). A strong sensitivity of liftoff height to N_2 dilution, jet velocity, and co-flow equivalence ratio is observed. Liftoff heights predicted by Kalghatgi's correlation are unable to capture the effects of N_2 dilution on liftoff height for the heated co-flow cases. A uniquely formulated Damköhler number, where the chemical time scale is based on flame propagation rather than autoignition, was therefore developed which acceptably captures the effects of jet velocity, nitrogen dilution and environment temperature on liftoff height. Satisfactory agreement between the correlation results indicate that stabilization is dominated by propagation, and prior studies with similar flames, such as the research of Muñiz and Mungal (1997) indicate that the propagating flame is likely tribrachial.

Keywords: Hydrogen; jet flames; turbulent combustion; flame propagation; autoignition

Introduction

Carbon Capture and Sequestration (CCS) provides a means of generating power from fossil fuels without emitting Carbon Dioxide (CO_2) into the atmosphere. One CCS technology of particular interest is called pre-combustion CCS where hydrogen (H_2) is produced through gasification or pyrolysis of fossil fuels which can be used as a fuel in gas turbine combustors, for instance [1]. In comparison with the natural gas widely utilized in current state-of-the-art gas turbines, H_2 is characterized by a much greater energy density by mass. However, the significantly reduced autoignition delay times of preheated H_2 mixtures, wide flammability limits, and high flame speeds, imply that current gas turbine combustors are not optimized for H_2 operation. Of the many challenges in developing lean premixed, partially premixed, and non-premixed H_2-fired gas turbines [2], one of the most serious fundamental issues is the stabilization of lifted H_2 jet flames, where both an improved understanding and characterization of data sets is needed.

Several theories exist which propose explanations of the mechanism responsible for stabilizing turbulent lifted jet flames [3, 4], including premixed flame propagation [5], the extinction of diffusional flamelets [6, 7], large scale structures [8], tribrachial flame behavior [9, 10], and autoignition [11, 12, 13, 14] when a heated co-flowing oxidizer is included. Markides et al. (2005) [15] also experimentally investigated the effects of turbulence interactions between the jet and surroundings on liftoff for autoignition dominated flames and concluded that these processes are coupled and that turbulent mixing between the jet and co-flow delays autoignition.

Despite the myriad of flame stabilization theories in existence, a simple correlation proposed by

---

* Corresponding author. E-mail: northodox@gmail.com

Kalghatgi [16] which relies solely on the premixed flame propagation theory as the flame stabilization mechanism, is capable of reproducing virtually all turbulent lifted jet flame data including those with Nitrogen (N$_2$) dilution, yet importantly, excluding cases where a vitiated co-flow has been applied. Peters (2000) [17] explains that for the "conventional" lifted turbulent jet flames the Damköhler number is small enough for premixed flame propagation terms to dominate over terms related to the extinction of laminar diffusional flamelets. Peters further argues that the flame structure observed with these flames (without heated co-flows) is commonly tribrachial, though the liftoff height (L) is often governed by multiple stabilization mechanisms while consistently enhanced by tribrachial flame geometry [17]. It should also be noted that while laminar diffusion quenching events do not determine the liftoff height, there is little doubt that diffusion flame quenching is responsible for the liftoff of an initially attached flame [17]. When local fluctuating strain rates near the nozzle exceed a threshold value, the flame is forced downstream where scalar dissipation rates are relaxed and mixing lengths are increased. The influence of scalar dissipation on flame stabilization is further explained by Peters [7]. The stabilization region, however, is on average downstream of the region where local scalar dissipation rates descend below the threshold quenching value because of insufficient tribrachial flame speeds. Instead, the flame stabilizes at a radius and axial location where the speed of an ensemble of tribrachial flamelets balances the local flow velocity. Kalghatgi's correlation is capable of accounting for tribrachial flame speed enhancement through calibration of the constant of proportionality, which is also fuel dependent.

Predicting the liftoff height of lifted turbulent jet flames is arguably the most severe model validation test [17], hence liftoff height characterization data have been used in the development and validation of many sophisticated models. Some example models include application to turbulent lifted H$_2$-in-N$_2$ jet flames in vitiated co-flows and in describing the flame stabilization mechanism at work. Cao et al. (2005) [18] used the joint velocity-turbulence frequency-composition PDF method and captured the strong sensitivity of liftoff height to co-flow temperature that is observed in experimental results. They also found that model results suggest that flame stabilization is primarily controlled by chemical kinetics for the flames studied. Additionally, Kumar et al. (2007) [19] used a flame extinction model based on the k-ε turbulence time scale concept for the prediction of liftoff heights for a wide variety of conditions and fuels including cases with hot co-flows. Kumar et al. observed that the flame stabilizes where the

local flame propagation speed equals the local fluid velocity. The same method was also used to predict combustion dynamics for mild combustion burners [19].

Since experimental data sets of turbulent lifted jet flames are critical for numerical model development and validation, extensive work is being conducted to broaden these data sets. Gordon et al. [20-23] recently made significant experimental contributions involving turbulent H$_2$-in-N$_2$ jet flames in a vitiated co-flow. A primary motivation for their work was the determination of a means of differentiating between regimes dominated by partially premixed flame propagation from those dominated by autoignition. Co-flow temperatures between 1000 K and 1475 K were considered, and the dependence of liftoff height on co-flow temperature ($T_{co-flow}$), co-flow velocity, and jet velocity (V_{jet}) was characterized. They concluded that the liftoff height for hydrogen jet flames is more sensitive to co-flow temperature than that of methane lifted jet flames owing to the aforementioned greater H$_2$ autoignition sensitivity versus that of methane.

The present work is similar to the work by Gordon et al. (2005) [20-23], though the motivations are distinct and the approach here is unique and beneficial. The nature of flame stabilization is investigated experimentally using an upgraded Berkeley Vitiated Co-flow Burner (VCB) [24] as sketched in Fig. 1. The reason for choosing Berkeley's VCB configuration is twofold. Firstly, the VCB represents a convenient setup for a parallel experimental and numerical investigation. Secondly, the VCB allows relatively simple and well defined specifications of the boundary conditions together with straightforward measurements of the main parameter (L). Thirdly, the VCB presents an opportunity for investigating the chemical kinetic complications inherent when recirculation is involved as well as the complications involved with high Reynolds number turbulence. Recirculation occurs with the VCB as a result of the high shear forces between the jet reactants and the co-flow products. Finally, the VCB configuration is also relevant to applications; it in fact represents a compact and geometrically simplified version of the Alstom GT24/26 second stage burner (Sequential EV), as described in [32].

The VCB consists of an ambient temperature high velocity fuel jet issuing into a co-flowing stream containing nearly adiabatic products of lean premixed H$_2$-air combustion. The geometry of the upgraded VCB (in comparison to the original design by Ricardo Cabra [11]) is designed to increase the operational flexibility of the burner allowing investigations of broader V_{jet} and nitrogen dilution mole fractions (y_{N2}) ranges, and for better co-flow fluidic

control without prohibitively complicated flow control techniques. The jet inner diameter has been scaled down by a ratio close to the co-flow dimension downscaling factor in preserving the 'potential core' height [25], which is the height at which outside air entrainment begins. Cabra et al [25] measured the potential core height on the original burner reporting z/d = 42, which is greater than the liftoff heights encountered with the current burner. Similarity is invoked with the upgraded burner in making use of the potential core height measurements performed by Cabra et al. Additionally, the reduced co-flow temperatures investigated in the present research increases the potential core height [25]. The temperature of the co-flow stream is controlled by varying the co-flow stoichiometry ($\varphi_{co\text{-}flow}$). N$_2$ is added to the fuel jet which encourages the flame to lift from the nozzle by increasing scalar dissipation rates near the nozzle which quenches the combustion reaction locally [7]. Chemical kinetic effects also likely play an important role on the effect of N$_2$ dilution on flame detachment, though research by Karbassi et al. [26] shows that the molecular mass of the diluent added to the fuel plays a most critical role on attached flame stability. Hence, the impact of N_2 addition is likely dominated by the effect of momentum effects independent of V_{jet} adjustments.
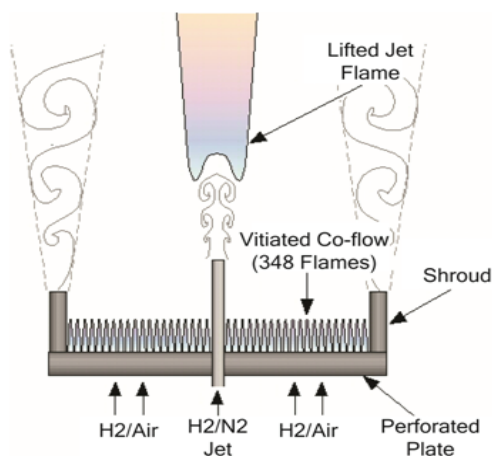

Fig. 1. Berkeley's VCB used in developing experimental data.

In the current research, flame stability is characterized experimentally by creating stability regime diagrams which outline the conditions under which the flame is attached, lifted, blown-out or unsteady. The lifted regime is further experimentally investigated, and the dependence of L on V_{jet}, y_{N2}, and $\varphi_{co\text{-}flow}$ is characterized. The range of operating conditions investigated is broader than prior experimental investigations, allowing an improved understanding

of how the stability mechanisms change as functions of operating conditions. The jet diameter (2.4 mm) is smaller than many prior studies. A small diameter jet affects the range over which stable lifted flames exist, while allowing a broad range of jet velocities to be studied with practical flow control mechanisms. Contrary to studies of conventional jet flames (e.g., those with no co-flow), the heated co-flow employed in the current research (along with other aforementioned studies) allows for the possibility of a different flame stabilization mechanism due to increased Damköhler numbers.

The increased Damköhler number promotes terms other than those dominated by flame propagation; terms which were not included by Peters [17] in analyzing flames at atmospheric pressures. Instead, it is possible for autoignition to play a more dominant role than flame propagation at higher temperatures ($T_{co\text{-}flow}$ > 800 K) [15] yet the exact nature of flame stability at intermediate temperatures (600 K – 800 K) is not as well characterized. Generally speaking, a combination of (tribrachial) flame propagation and autoignition processes could be influential over the range considered. Since several stability mechanisms are likely influential when the entirety of the independent parameter space in the current research is considered, no attempt is made here to improve the theoretical understanding of the individual flame stabilization theories nor is any attempt made to propose a new theory. Instead, attempts are made at identifying the conditions under which existing theories apply in various regions of the stability regimes diagrams. Moreover, the current research is intended to provide a broad experimental data set for numerical model benchmarking. The numerical models can subsequently be used for applications where many flame stabilization mechanisms are influential and in assisting the modeling community in determining the conditions under which particular numerical methods are applicable and when they are not.

Experimental and Numerical Methods

Experimental Methods

VCB Design

The VCB consists of a high velocity jet issuing into hot co-flowing products of lean combustion, as shown in Fig. 1. The inner diameter of the jet is d_{jet} = 2.4 mm, the outer diameter of the jet is d_o = 6.4 mm, and the outer diameter of the co-flow is D_o = 9.7 cm. The co-flow is generated with a perforated plate consisting of 348 (1.6 mm diameter) holes drilled into a 9.5 mm thick brass plate arranged in a hexagonal pattern with 4.8 mm separation between holes,

and an overall blockage of 89%. The jet nozzle extends 25 mm above the base of the co-flow burner plate, and a 19 mm tall shroud is placed around the co-flow which reduces outside air entrainment while maintaining visibility of the jet nozzle. A blunt-edge nozzle (also known as a squared-off nozzle) is used because early scoping work indicates that changing from a blunt edge nozzle to a tapered nozzle bears no discernible impact on the liftoff height L, which is the primary focus of the research. It is assumed that the insensitivity of liftoff height on nozzle geometry occurs because the liftoff heights generated with this burner configuration are sufficiently far away from the nozzle ($L/d \geq 10$ in all cases) for negligible liftoff height contributions from local recirculation effects around the nozzle exit. Since a blunt-edge nozzle facilitates modeling (primarily because meshing a square nozzle is significantly less complicated), a square nozzle is used here. Thin walled tubes are avoided in reducing heat transfer from the co-flow products to the jet reactants. Simple 1D heat transfer calculations where performed which show that even with the most conservative assumptions (1. outer wall tube temperature equaling the greatest co-flow temperature investigated of 1200 K, 2. pure hydrogen fuel, 3. a minimum jet velocity of 300 m/s), the fuel temperature would rise by only 28 K. The conservative nature of the assumptions invoked with this calculation indicates that fuel temperature increases in the jet nozzle are negligible.

Scope of Operational Conditions

The operational conditions investigated include co-flow equivalence ratios of $0.00 \leq \varphi_{co-flow} \leq 0.35$ (corresponding to co-flow temperatures of 293 K $\leq T_{co-flow} \leq 1200$ K) and jet N₂ mole fractions of $0.0 \leq y_{N2} \leq 0.55$. For all experiments, the jet fuel temperature is approximately $T_{jet} \approx 293$ K and the co-flow bulk velocity before combustion is held constant at $u_{co-flow} = 0.67$ m/s (7.3 m/s in the holes in the plate). The co-flow velocity of the combusted products of the lean premixed flame ranges from roughly 0.67 m/s (for co-flowing air) to roughly 3.2 m/s (for $T_{co-flow} = 1200$ K). Co-flow temperatures are estimated using an experimentally developed correlation [25] of the form:

$$T_{co-flow} \text{ (K)} = 2462(\varphi_{co-flow})^{0.69} \qquad (1)$$

Equation 1 was developed for $0.15 \leq \varphi_{co-flow} \leq 0.5$ and accounts for non-adiabatic conditions. The correlation was based on Raman-Reyleigh thermometry measurements with a reported uncertainty of 3% versus the uncertainty correlated with thermocouple measurements of 5%. Thermocouple measurements

performed with the upgraded apparatus also fall within the 5% uncertainty value. The co-flow blowoff limit with the upgraded burner is in agreement with the co-flow blowoff limit observed here, and the burner design is scale similar with Cabra's original design. Thus, there exists greater confidence in the accuracy of the correlation developed by Cabra et al. over thermocouple measurements and this correlation is consequently opted for co-flow temperature characterization in lieu of thermocouple measurements.

The speed of sound in pure H₂ is ~1300 m/s. As N₂ dilution is increased, however, the speed of sound in the jet fluid decreases. For example, for the case with the maximum amount of N₂ dilution investigated in the current work ($y_{N2} = 0.55$), the speed of sound in the jet fluid is ~500 m/s. Consequently, it is not possible to achieve N₂ dilution values greater than 0.55 with the jet nozzle used. Additionally, compressibility effects are critical for high y_{N2} values and should be included when modeling flames with high y_{N2} values.

Stability Regime Diagrams Development Methodology

Stability regime diagrams are created for $V_{jet} = 300$, 400, and 500 m/s. $\varphi_{co-flow}$ is held constant for a given experiment, and y_{N2} is slowly increased until the flame lifts or becomes unsteady, which allows the point of transition (from attached to lifted and lifted to blown-out) to be recorded. The unsteady regime, in the context of this research, is characterized by repeated transitions from an attached condition to a lifted condition where the liftoff height rapidly increases until blowout, and subsequent rapid ignition of the jet reactants. When re-ignition occurs, an attached flame is again formed and the cycle is repeated. It is important to note that hysteresis effects in influencing the transition to the lifted condition are well known and documented [3], and the boundary between the attached flame and a lifted flame is different when y_{N2} is ramped down instead of ramped up. (e.g., when a flame is already lifted, reducing y_{N2} yields a lifted flame for values of y_{N2} where an attached flame is present if starting from an attached flame and increasing y_{N2}). Nonetheless, a single stability regime diagram for each case is desired for bounding the liftoff height characterization portion for the current research so each experiment starts from an attached flame and y_{N2} is increased until the flame lifts in simplifying the liftoff height characterization which follows. The nitrogen ramping scheme, however, does not affect jet flame stability characteristics in the unsteady regime for the current burner geometry. A sweep of $\varphi_{co-flow}$ values of

interest is investigated and the data forms the stability regime diagrams which summarize the conditions under which the flame is attached, lifted, blown-out and unsteady when y_{N2} dilution is ramped up.

Liftoff Height Characterization Methodology

Liftoff height L is determined by measuring a time averaged ensemble of schlieren images (see Fig. 2) with a shutter time of 156 µs. The liftoff height definition is relatively unambiguous at this frame rate and is defined as the location where the schlieren image depicts a noticeable density gradient in the jet stream. The schlieren imaging approach is advantageous over direct imaging as prior research where direct imaging was employed and uncertainty values were computed demonstrated that the magnitude of uncertainty resulting from the long frame rates required with direct imaging are often the same order of magnitude as the liftoff height measurements themselves [28]. In the current research, 50 frames equally spaced apart in a period of 10 seconds were analyzed by hand in determining the mean liftoff height. All experiments are conducted at atmospheric pressure.
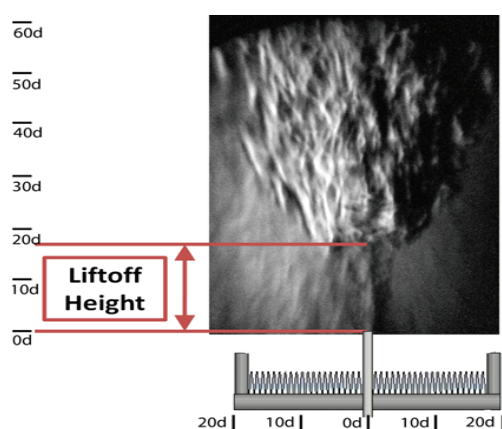

Fig. 2. Example schlieren image depicting a lifted N_2-in-H_2 jet flame showing qualitatively how the liftoff height is defined.

While the effect of this broad range of independent parameters on liftoff height is presented, results are shown with y_{N2} on x-axes instead of $\varphi_{co\text{-}flow}$ or V_{jet} because the dependence of L on y_{N2} appears linear, which is not always the case with $\varphi_{co\text{-}flow}$ and V_{jet}. Liftoff height measurement results demonstrate that when 3 independent parameters are made variable, significant scatter in liftoff heights result which is a significant modeling challenge. Development of a robust correlation which describes the liftoff height dependence on y_{N2}, V_{jet} and $\varphi_{co\text{-}flow}$ is also challeng-

ing. RMS values, minimum and maximum values, and a PDF of the liftoff heights, while extremely useful, are not included in the present research because the manual nature by which of liftoff heights are measured makes these additional statistical determinations prohibitively time intensive.

Numerical Methods

Flame speed, S_L, flame thickness, δ, and the corresponding chemical timescale corresponding to mixtures of jet reactants and co-flow products are calculated using Chemkin II PREMIX [27]. In PREMIX, mixtures of the jet and co-flow are pre-calculated and used as inputs which determined an overall global equivalence ratio ($\overline{\varphi}_{Global}$). Note that $\overline{\varphi}_{Global}$ is distinct from $\varphi_{co\text{-}flow}$. Mixture averaged properties are assumed. The flame thickness is defined as the region between 10% and 90% of the temperature difference between the burned and unburned sides of the premixed flame. An example computation set of S_L versus $\overline{\varphi}_{Global}$ for cases with $\varphi_{co\text{-}flow}$ fixed at 0.18 for four selected y_{N2} values is presented in Fig. 3. A relationship between the laminar flame speed S_L, the mean local equivalence ratio $\overline{\varphi}_{Global}$ and y_{N2} is fit to the form $S_L(\overline{\varphi}_{Global}) = \alpha\,\overline{\varphi}_{Global}{}^{b}\,exp(\text{-}c\,(\overline{\varphi}_{Global} - d))$ using data computed from PREMIX. The constants a, b, c and d are functions of y_{N2}. Note that the unburned mixture temperature varies with $\overline{\varphi}_{Global}$. The detailed H_2 chemical kinetic mechanism from Li et al. (2004) [30] [-36958940] is used for all numerical simulations and equilibrium $T_{co\text{-}flow}$ and compositions are assumed. The fitting relation matches the computed laminar flame speed well, with average error around 10% overall and with lower errors are observed for the regions of interest. The chemical timescale is defined as the ratio of δ to S_L and is hereafter referred to as the flame time. The computed flame time values are used in correlating experimental data.
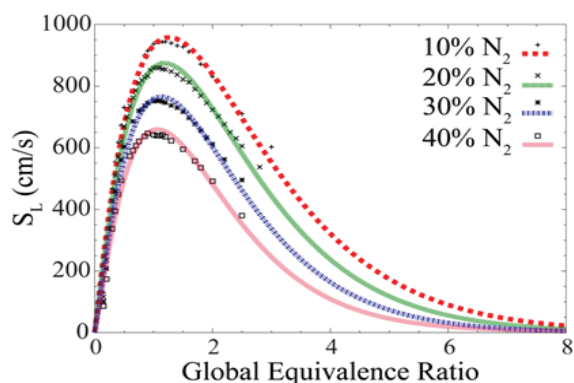

Fig. 3. Computed laminar flame speeds versus jet N_2 dilution and global equivalence ratio and the correlation results plotted alongside (solid lines) for an example case with $\varphi_{co\text{-}flow}$ = 0.18.

Results and Discussion

Stability Regimes Development

Figure 4 presents stability regime diagrams produced from the data for V_{jet} = 300 m/s, 400 m/s and 500 m/s with $\varphi_{co-flow}$ (and hence $T_{co-flow}$) and y_{N2} as the two independent parameters. Results are illustrated with $\varphi_{co-flow}$ on the primary x-axis and with the correlated $T_{co-flow}$ determined from Eq. 1 on the secondary x-axis. As shown in Fig. 4, four distinct regions of the stability regime diagrams are identified; an attached flame, a lifted flame, a blown-out flame and an unsteady flame. For $\varphi_{co-flow}$ < 0.15, the co-flow is blown-out (does not remain lit), thus no data points are generated in the region between $0 < \varphi_{co-flow} < 0.15$. A stability regime is drawn for $0 < \varphi_{co-flow} < 0.15$ nonetheless in allowing placement of a label of the lifted regime for the low V_{jet} cases where the actual lifted regime is small. Therefore the stability limits for $0 < \varphi_{co-flow} < 0.15$ are implied and not measured. The dashed line for the V_{jet} = 500 m/s cases indicates the boundary between the lifted and unsteady regimes.
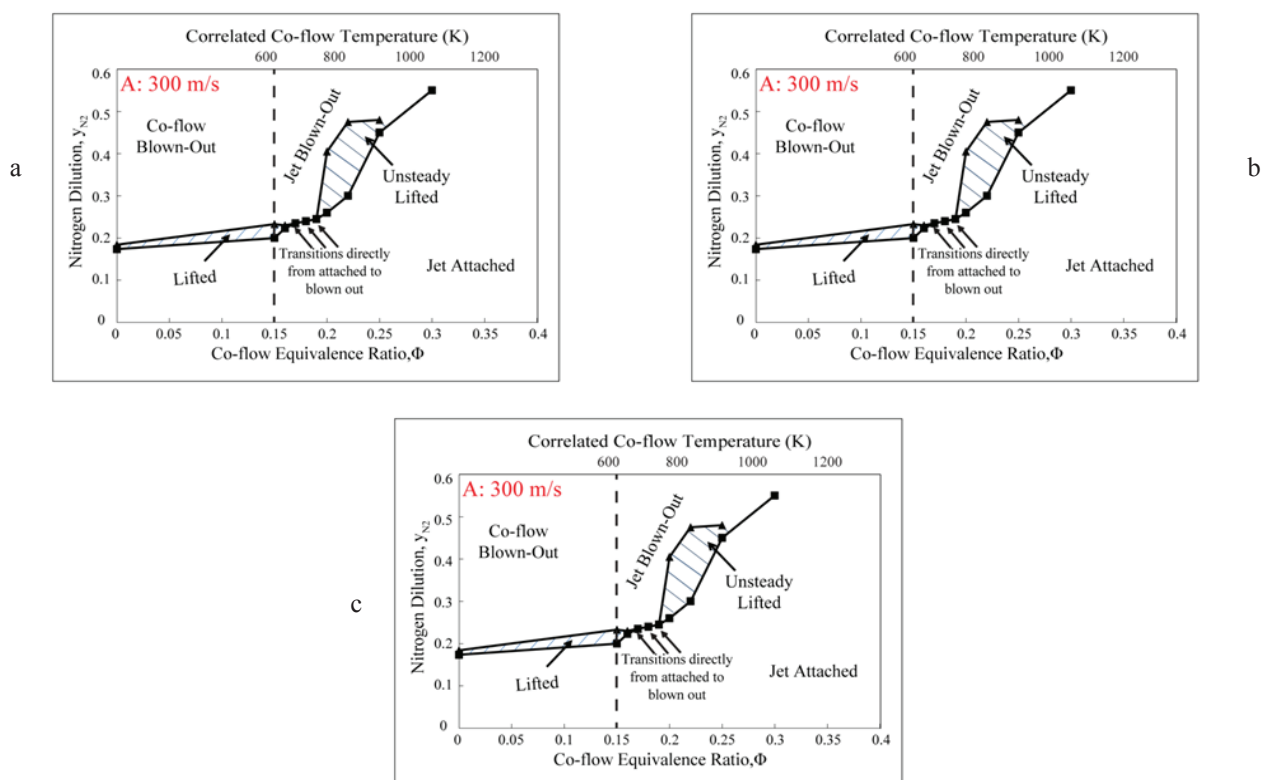
Fig. 4. Stability regimes Diagrams which map the flame stabilization behavior for V_{jet} = 300 m/s (a), V_{jet} = 400 m/s (b) and 500 m/s (c).

In the lifted regime, the transition from attached to lifted is abrupt. For y_{N2} values immediately below the lifted regime transition, no visible indicators that the flame is nearing liftoff are observable. Similarly, in the unsteady regime, the transition from attached to unsteady is abrupt so these transitions are easily delimited. At lower jet velocities and for $0.15 \le \varphi_{co-flow} \le 0.20$, the jet transitions from an attached flame to a blown-out one, with no lifted region. Increasing the jet velocity broadens the lifted regime for $0.15 \le \varphi_{co-flow} \le 0.20$. As explained in section 2.2, for $\varphi_{co-flow}$ < 0.20 the co-flow temperature is below the autoignition temperature, meaning that the temperature of any mixture between the fuel (at 293 K) and co-flow (300 K for air at $\varphi_{co-flow}$ = 0 and 810 K for $\varphi_{co-flow}$ = 0.20) is below the autoignition temperature. Therefore autoignition cannot be the sole flame stabilization mechanism, and tribrachial flame propagation is likely influential for $\varphi_{co-flow}$ < 0.20. As $T_{co-flow}$ surpasses the autoignition temperature (near and beyond $\varphi_{co-flow}$ > 0.20), increasingly greater y_{N2} values are necessary for jet detachment. For example, Fig. 4c shows the stability regime diagram for V_{jet} = 500 m/s. The slope of the boundary line between attached and lifted regimes for $0.15 < \varphi_{co-flow}$ < 0.20 is much shallower than the slope of the

regime boundary line for $\varphi_{co\text{-}flow} > 0.20$. For $\varphi_{co\text{-}flow} > 0.20$ with increasing y_{N2}, the jet no longer transitions from attached to lifted, but rather from attached to unsteady. Had y_{N2} been ramped down instead of up, the attached-lifted boundary is slightly reduced owing to hysteresis. However, the stability boundaries in the unsteady regime are unaffected by hysteresis. Cases where y_{N2} are ramped down are not investigated extensively for simplicity since the primary focus of this research is on analyzing liftoff height variation in the lifted regime. Stability hysteresis on $\varphi_{co\text{-}flow}$ and V_{jet} slightly affect the stability regimes layout, though for the burner configuration used, stability is most sensitive on y_{N2}, so these hysteresis effects are likely less influential than hysteresis on y_{N2}. Additionally, $\varphi_{co\text{-}flow}$ and V_{jet} are fixed in the development of the stability regimes diagrams in reducing the impacts of hysteresis on $\varphi_{co\text{-}flow}$ and V_{jet}.

The relatively small inner diameter of the jet used (2.4 mm) leads to high strain with weak tribrachial characteristics which prohibits stable lifted flames when $\varphi_{co\text{-}flow} > 0.20$. Peters [17] explains why diffusion flame quenching is responsible for the liftoff of an initially attached flame. When the jet diameter is smaller than the threshold value (~3 mm, above which liftoff height is linearly dependent on jet velocity) laminar diffusional flamelet quenching drives the stabilization point beyond the threshold liftoff height of $L = 40$ diameters, resulting in flame instability. Consequently, for $\varphi_{co\text{-}flow} > 0.20$, stable lifted flames cannot be generated with the burner configuration used since the co-flow temperature is greater than the autoignition temperature. However, the jet is capable of reigniting once an autoignition event strong enough for full jet ignition becomes favorable, and the cycle is repeated [36]. The frequency of these ignition and subsequent blow-off events ranges between 0 Hz and 30 Hz depending on V_{jet}, $\varphi_{co\text{-}flow}$, and y_{N2}. The stability regimes diagrams serve as a convenient tool for predicting H_2-in-N_2 flame behavior under various conditions and for analyzing the numerical and experimental results when available.

Liftoff Height Characterization

Concurrently in the development of the stability regimes diagrams, the liftoff heights under the same conditions were measured using the methodology outlined in section 2.1. Figure 5 summarizes these results. Note that the liftoff height results presented are fundamentally distinct from those measured by Cabra et al. [11] as the co-flow temperature ranges investigated do not overlap between the present research and Cabra's work and because of the afore-

mentioned fluid dynamic effects resulting from the jet nozzle diameter adjustment. At any fixed V_{jet} and y_{N2} condition, a marked difference in liftoff heights is not observed as the co-flow equivalence ratio is increased beyond $\varphi_{co\text{-}flow} = 0.15$ ($T_{co\text{-}flow} = 660$ K) until $\varphi_{co\text{-}flow} = 0.20$ ($T_{co\text{-}flow} = 810$ K). Above $\varphi_{co\text{-}flow} = 0.20$, autoignition is likely the dominant flame stabilization mechanism, which explains the differing liftoff heights for $\varphi_{co\text{-}flow} = 0.20$. Furthermore, a maximum non-dimensional liftoff height of approximately $L/d_{jet} \approx 24$ is observed. These results suggest that in practical combustors, when H_2 mixes with products originating at equivalence ratios near 0.20, numerical models which incorporate autoigniton and flame propagation should for optimal model accuracy. Figure 5 also demonstrates the significant degree of scatter in liftoff heights which results when 3 independent parameters are varied.
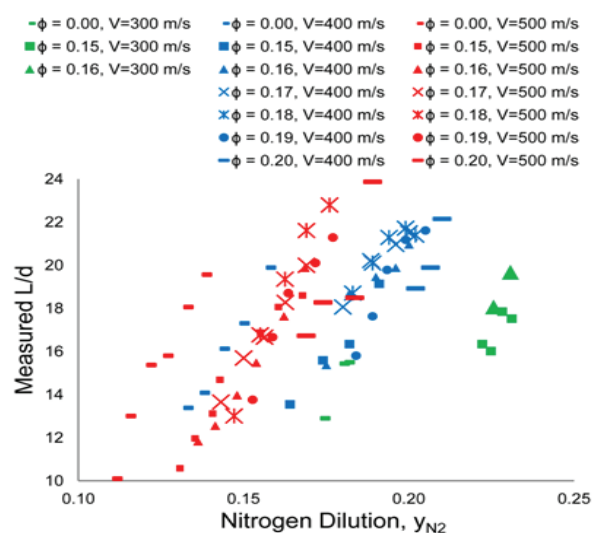

Fig. 5. Experimentally measured liftoff heights versus N_2 dilution for various jet velocities and co-flow equivalence ratios.

Liftoff Height Data Reduction

Kalghatgi's Correlation

The liftoff height in the steady lifted regime is investigated in detail ($0.15 < \varphi_{co\text{-}flow} < 0.20$). First, Kalghatgi's correlation [16] is used in investigating whether the correlation can accurately capture the influence of varying y_{N2} on L while the $\varphi_{co\text{-}flow}$ is varied:

$$L = 50 \frac{v_{jet} V_{jet}}{S_{L,\max}^2} \left(\frac{\rho_{jet}}{\rho_\infty} \right)^{1.5} \qquad (2)$$

where v_{jet} is the kinematic viscosity of the jet, ρ_{jet} is the density of the jet, and ρ_∞ is the ambient density (co-flow density). Kalghatgi's correlation has been previously shown to accurately predict liftoff heights for hydrocarbon jet flames, H_2 jet flames, and H_2 jet flames diluted with hydrocarbons and CO_2 [38]. However, note that Kalghatgi did not have a co-flow, heated or otherwise, in developing the correlation.

    Measured liftoff heights are plotted against those predicted by Kalghatgi's correlation with the jet mixture kinematic viscosity calculated using the methodology outlined in a NASA Technical Note by R.S. Brokaw [39]. Results of the comparison between measured results and those predicted by Kalghatgi's correlation are shown in Fig. 6. These results indicate that Kalghatgi's correlation correctly predicts the range of liftoff heights, but has trouble accurately predicting the effect of y_{N2} with a hot co-flow. Figure 7 shows Kalghatgi's correlation versus y_{N2} for the cases investigated. For hot co-flow cases ($\varphi_{co\text{-}flow} \geq 0.15$) Kalghatgi's correlation predicts only a weak dependence of L on y_{N2} whereas a strong dependence was observed experimentally. For the cold co-flow cases ($\varphi_{co\text{-}flow} = 0.00$), Kalghatgi's correlation shows better agreement with the experimental data for increasing y_{N2}. Discrepancies for the cold co-flow cases are attributable to the influence of the co-flow velocity on forcing the stabilization zone downstream, as explained by Montgomery et al. [40]. Despite the accuracy of Kalghatgi's correlation [38] without a co-flow, these results imply that for heated environments, caution should be used when applying the correlation.

Fig. 7. Liftoff height predictions from Kalghatgi's correlation versus N_2 dilution for the conditions investigated experimentally.

Normalization by Damköhler Number

    Prior work [41, 42] suggests that the Damköhler number definition derived from large-scale turbulence quantities is equally applicable to small-scale turbulence quantities, and vice versa. In taking advantage of this hypothesis, the Damköhler number is used in investigating whether liftoff heights can be characterized solely by this parameter. The Damköhler number is computed using two methods, both utilizing density weighting [43] in computing an effective velocity near the flame. The first Damköhler number definition Da_1 uses the jet diameter for computing the flow time scale:

$$Da_1 = \frac{\tau_{flow}}{\tau_{chem}} = \frac{d_{jet}(v_{jet}(\rho_{jet}/\rho_\infty)^{1/2})}{\delta/S_L} \qquad (3)$$

where τ_{flow} is the flow time scale, τ_{chem} is the chemical time scale, S_L is the flame speed, and δ is the flame thickness. An example τ_{chem} computation set is shown in Fig. 8, with $\overline{\varphi}_{Global}$ (equivalence ratios encountered as the jet reactants mix homogeneously with co-flow products) on the x-axis and the laminar flame speed (S_L), the flame thickness (d), and the flame time (τ_{chem}) on the y-axes. τ_{chem} and d share the same y-axis on the right hand side of Fig. 8 because the order of magnitude of the values are similar, so the units are given next to the plot labels. The minimum flame time on the lean side (near $\overline{\varphi}_{Global} = 0.4$) is not used because as fluid from the jet moves downstream and is entrained by the co-flowing
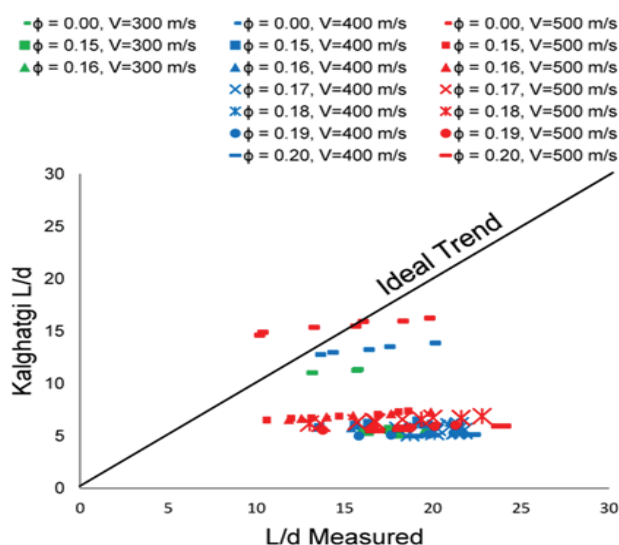

Fig. 6. Experimentally measured liftoff heights versus predictions computed using Kalghatgi's correlation for various jet velocities and co-flow equivalence ratios.
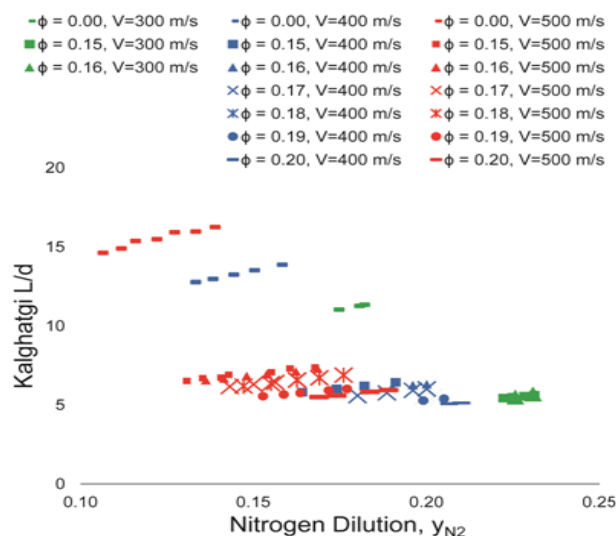
products, the mixture starts richer and become leaner. Consequently, the first minimum in chemical time scale that the mixture encounters is at a rich equivalence ratio. If the flame stabilized later, on the lean side, any downstream deviation from the stabilization point would move the flame toward an even leaner zone with a longer flame time. On the rich side, however, perturbations that move the stabilization zone downstream result in ignition compositions closer to stoichiometric where flame stability is enhanced. As a result, the flame time on the rich side is a stable minimum, whereas the minimum on the lean side is unstable.
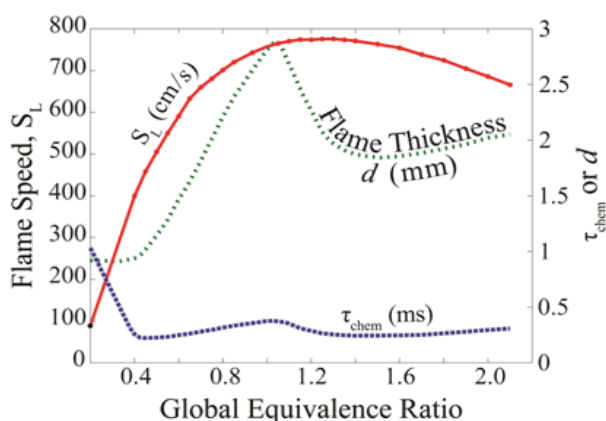

Fig. 8. An example calculation of the laminar flame speed, flame thickness, and flame time for $\varphi_{co\text{-}flow} = 0.18$.

$\overline{\varphi}_{Global}$ is determined through analysis of the global (1-step) reaction equation where equivalence ratio is set such that H_2/O_2 equals that of a reaction of H_2 with air at the same equivalence ratio. The resulting $\overline{\varphi}_{Global}$ definition can be computed using Eq. (4) for specified values of $\varphi_{co\text{-}flow}$, y_{N2}, and $y_{H2,G}$, where, $y_{H2,G}$ refers to the local (global) H_2 mole fraction as the jet reactants mix with co-flow products.

$$\overline{\varphi}_{Global} = \frac{0.5 + 2.38/\varphi_{co-flow}}{\left(1/y_{N_2,G} - \dfrac{y_{N_2,j}}{1-y_{N_2,j}} - 1\right)(1/\varphi_{co-flow} - 1)} \quad (4)$$

The jet diameter serves as a basis for the integral length scale, since turbulence scales cannot exceed the jet diameter before the jet fluid is issued into the environment. It is assumed here that a) the flame propagation speed scales with the laminar flame speed and that b) flame propagation is the mechanism most influential in determining the liftoff height for the steady lifted flames studied. The latter assumption is supported by Peters's work [17]. The former assumption is made with the understanding

that correlation scatter can be partially attributable to disparities between this assumption and the real conditions. The density weighting accounts for the influence of nitrogen dilution on jet momentum, independent of jet velocity [43]. As nitrogen dilution is increased, jet momentum increases, which increases downstream fluid velocities. Figure 9 is included as an example demonstrating the challenging task of correlation development of liftoff height for the conditions investigated.
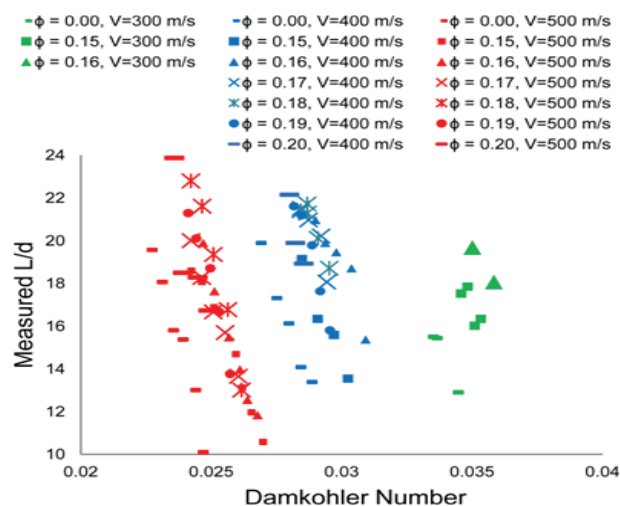

Fig. 9. Experimentally measured liftoff heights versus the Damköhler Number where the jet diameter is used as the flow length scale.

Damköhler Number Redefined

Because of the inadequacy of the traditional Damköhler number definition first employed, the Damköhler is redefined in more adequately accounting for the physics encountered with the VCB. The second method uses an alternative length scale in computing the flow time, $z_{\overline{\varphi}=1.5}$:

$$Da_2 = \frac{\tau_{flow}}{\tau_{chem}} = \frac{z_{\overline{\varphi}=1.5}/(v_{jet}(\rho_{jet}/\rho_\infty)^{1/2})}{\delta/S_L} \quad (5)$$

where $z_{\overline{\varphi}=1.5}$ is the axial location where $\overline{\varphi}_{Global} = 1.5$, which is where a flame time occurs as shown in Fig. 8 for an example case with $\varphi_{co\text{-}flow} = 0.18$. The assumption is made here that errors associated with using the z-location along the jet centerline versus the radial location (r_s) where stabilization actually occurs are negligible because r_s is typically small ($r_s = 1.7$ for the flame depicted in Fig. 2 for example) compared to the stabilization height. Scalar dissipation also impacts the stabilization location to a

degree, though Peters [17] explains that scalar dissipation effects are negligible when tribrachial propagation dominates.

Again, since flame propagation is deemed most influential in the stable lifted flames regime, τ_{flame} is used as the chemical time scale. The flow length scale modification is justifiable because the amount of time for the reactants to become ignitable (due to a decrease in scalar dissipation rate) is dictated solely by this length scale and by the fluid velocity (instead of the jet diameter and the fluid velocity). Furthermore, the jet diameter choice is incomplete because it does not allow for larger turbulence quantities to develop from a small jet which result from shear interactions with the co-flow.

Early research conducted by Birch et al. [45] on nonreacting jets issuing into quiescent environments resulted in a correlation relating local composition along the jet centerline with z. With this correlation, it becomes possible to modify the flow length scale to this more appropriate value in order to improve agreement with experimental results. The axial location which minimizes flame time, $z_{\overline{\varphi}=1.5}$, is calculated from:

$$z_{\overline{\varphi}=1.5} = \left[4 \frac{y_{jet}}{y_{\overline{\varphi}=1.5}} \left(\frac{\rho_{jet}}{\rho_\infty} \right)^{1/2} - 5.8 \right] d_{jet} \qquad (6)$$

where y_{jet} is the mass fraction of the fuel in the jet, is the mass fraction of the fuel for $\overline{\varphi}_{Global} = 1.5$, ρ_{jet} is the density of the jet, and ρ_∞ is the density of the ambient fluid (the co-flow). It is assumed here that the correlation for the centerline fuel concentration decay profile is unaffected by chemical reaction, and this assumption has been shown to be reasonably accurate [44] with reacting flows. The liftoff height data is then plotted against these Damköhler numbers in identifying a single functional relationship between Damköhler number and liftoff height.

The first method using the jet diameter in computing the flow time length scale (Fig. 9) captures the effects of N_2-in-H_2 dilution on L at fixed V_{jet}, but the results are functionally dependent on V_{jet} as this parameter is varied. The conclusion following this observation is that when inappropriate length or time scales are used in the Damkohler number definition, correlation results are not meaningful. The second method, however, captures the trend with good agreement regardless of $\varphi_{co-flow}$, V_{jet}, and y_{N2}. The result is shown in Fig. 10. This result suggests that the Da_2 formulation based on macroscopic features applies equivalently to the small scales in determining the stability point. The scatter is likely due to the fact that in some cases with higher $\varphi_{co-flow}$

values, autoignition is competing with propagation in stabilizing the flame as well as some contributions from compressibility effects. The satisfactory agreement is also an indicator that numerical models which do not include compressibility effects can produce meaningful results in the lifted regime.
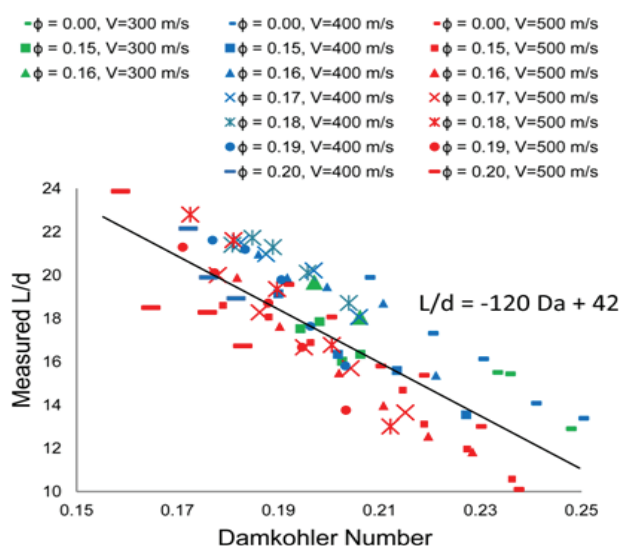

Fig. 10. Experimentally measured liftoff heights versus the Damköhler Number where the flow length scale is based on the axial location where the concentration of the fuel results in a minimum chemistry time.

A metric for determining how to incorporate the autoignition delay time into the Damköhler number formulation by the use of a weighted average of the flame time and an autoignition delay time which accounts for mixing between the jet and co-flow would likely improve agreement. The weighting percentages should appropriately incorporate the effect of $T_{co-flow}$ on the stabilization mechanism and the relative importance of autoignition versus tribrachial flame propagation. Additionally, a constant of proportionality that makes the flame time and delay time comparable in terms of how they influence L would likely reduce scatter in the results.

Conclusions

Stability regime diagrams are presented which outline the conditions under which a N_2-in-H_2 jet flame in a vitiated co-flow is attached, lifted, blown-out or unsteady. The stability regime diagrams are an effective means of facilitating understanding of the interaction of the factors influential in stabilizing jet flames. For the burner geometry used, it is found that lifted flames exist for co-flow equivalence ratios below 0.20 when enough N_2 dilution is added to the

fuel. A co-flow equivalence ratio of 0.20 corresponds to an estimated co-flow temperature of 810 K which is near the autoignition temperature of H_2 indicating that lifted flame stability is likely dominated by flame propagation for all cases where stable lifted flames exist. For co-flow equivalence ratios above 0.20, autoignition becomes important, and the flame is unsteady with no definable liftoff height.

The lifted flame regime is further characterized by determining the dependence of liftoff height on N_2 dilution, jet velocity, and co-flow equivalence ratio. Kalghatgi's correlation for predicting lift-off heights L, which shows excellent results for jets issuing into quiescent environments, is investigated in determining its applicability for cases where a heated co-flow is involved. Kalghatgi's correlation poorly predicts the trend for hot co-flow conditions, yet captures the trend adequately for cold co-flow conditions. Thus, the correlation is found incapable of predicting correctly the dependence of liftoff height on N_2 dilution for hot co-flows. Correlations found inappropriate where heated co-flows are applied and when the co-flow temperature remains below that which autoignition dominates flame stabilization motivate the development of a correlation which incorporates the temperature effect on propagating turbulent lifted flames. A new correlation based upon the Damköhler number, with careful selection of flow and chemical time scales is developed in investigating the performance of this correlation for the conditions investigated. The liftoff height data is plotted against the Damköhler number showing a direct relationship when the Damköhler number is appropriately defined. This result suggests that the Damköhler number is an overarching parameter that describes lifted flame dynamics for the conditions investigated, which span many flame stabilization regimes. By properly choosing the parameters defining the turbulence time scales and chemical time scales which address the dominant flame stabilization mechanism, a linear dependence of liftoff height on the Damköhler number is observed. Consequently, the Damköhler number can be used as a means of estimating the liftoff height when experimental data is nonexistent for guiding future experimental and numerical work. This result reinforces the hypothesis that flame propagation dominates flame stabilization for these flames when the co-flow is below the autoignition temperature. Numerous prior studies indicate that for lifted flames in ambient environments, tribrachial flame propagation is paramount, and may also be paramount for these flames. For stable lifted flames issuing into co-flows hotter than the autoignition temperature, autoignition becomes influential in determining the ignition location. For these flames, the Damköhler number should incorporate the autoignition delay time into the chemical time scale instead of using the flame time alone. The potential for using a single metric for predicting liftoff characteristics across several stability regimes, however, is attractive.

Acknowledgements

References

[1]. O. Bolland, H. Undrum, Advances in Environmental Research 7 (2003) 901–911.
[2]. P. Chiesa, G. Lozza, L. Mazzocchi, ASME J. of Eng. Gas Turbines and Power 127 (2005) 73–80.
[3]. K.M. Lyons, Prog. Energy Combust. Sci. 33 (2007) 211–231.
[4]. W.M. Pitts, Proc. Combust. Inst. 22 (1988) 809–816.
[5]. L. Vanquickenborne, A. Van Tiggelen, Combust. Flame 10 (1966) 59–69.
[6]. M.J. Dunn, A.R. Masri, R.W. Bilger, R.S. Barlow, G.H. Wang, Proc. Combust. Inst. 32 (2009) 1779–1786.
[7]. N. Peters, F.A. Williams, AIAA 21 (3) (1983) 423–429.
[8]. M.M. Tacke, D. Geyer, E.P. Hassel, J. Janicka, Proc. Combust. Inst. 27 (1998) 1157–1165.
[9]. L. Muniz, M.G. Mungal, Combust. Flame, 111 (1997) 16–31.
[10]. Buckmaster, J. Prog. Energy Combust. Sci. 28 (2002) 435–475.
[11]. R. Cabra, T. Myhrvold, J.Y. Chen, R.W. Dibble, A.N. Karpetis, R.S. Barlow, Proc. Combust. Inst. 20 (2002) 1881–1888.
[12]. R. Cabra, J.Y. Chen, R.W. Dibble, A.N. Karpetis, R.S. Barlow, Combust. Flame 143 (2005) 491–506.
[13]. T. Myhrvold, I.S. Ertesvag, I.R. Gran, R. Cabra, J.Y. Chen, Combust. Sci. Technol. 178 (2006) 1001–1030.
[14]. R.L. Gordon, A.R. Masri, S.B. Pope, G.M. Goldin, Combust. Theory Model. 11 (3) (2007) 351–376.

[15]. C.N. Markides, E. Mastorakos, Proc. Combust. Inst. 30 (2005) 883–891.

[16]. G.T. Kalghatgi, Combust. Sci. Technol. 41 (1984) 17–29.

[17]. N. Peters, Turbulent Combustion, Cambridge University Press, Cambridge, U.K., 2000, 237-261.

[18]. R.R. Cao, S.B. Pope, A.R. Masri, Combust. Flame 142 (2005) 438–453.

[19]. S. Kumar, P.J. Paul, H.S. Mukunda, Combust. Sci. Technol. 179 (2007) 2219–2253.

[20]. R.L. Gordon, S.H. Stårner, A.R. Masri, R.W. Bilger, Further Characterisation of Lifted Hydrogen and Methane Flames Issuing into a Vitiated Co-flow, 5th Asia-Pacific Conference on Combustion, Asia-Pacific Regional Affiliate of the Combustion Institute, Adelaide, Australia, 2005.

[21]. R. Gordon, A. Masri, E. Mastorakos, Combust. Flame 155 (2008) 181–195.

[22]. R. Gordon, A. Masri, S. Pope, G. Goldin, Combust. Flame 151 (2007), 495–511.

[23]. R. Gordon, Ph.D. thesis, The University of Sydney, 2007.

[24]. R. Cabra, Turbulent Jet Flames in a Vitiated Co-flow, Report No. NASA/CR-2004-212887 E-14301, NASA Glenn Research Center, 2004.

[25]. R. Cabra et al, Turbulent Jet Flames into a Vitiated Coflow. PhD Thesis, UC – Berkeley 2005.

[26]. M. Karbassi, I. Wierzba, J. Energy Resource Technol. 120 (1997) 167–171.

[27]. R. Kee, J. Grcar, M. Smooke, J. Miller, SAND85-8240. (1985).

[28]. P.R. Medwell, B.B. Dally, Energy and Fuels. 26 (2012) 5519–5527.

[29]. J.Y. Chen, W.C. Chang, Combust. Sci. Technol. 133 (1998) 343–375.

[30]. J. Li, Z. Zhao, A. Kazakov, F.L. Dryer, Int. J. Chem. Kinet. 36 (2004) 566–575.

[31]. J. Ströhle, T. Myhrvold, Int. J. Hydrogen Energy 32 (2007) 125–135.

[32]. K. Döbbeling, J. Hellat, H. Koch, ASME J. Eng. Gas Turbines and Power 129 (2007) 2–12.

[33]. P. Patnaik, A Comprehensive Guide to the Hazardous Properties of Chemical Substances, Wiley-Interscience, Hoboken, New Jersey, U.S., 2007 402.

[34]. J.Y. Chen, W. Kollmann, Proc. Combust. Inst. 22 (1989) 645–653.

[35]. S. Muppala, J.X. Wen, N.K. Aluri, F. Dinkelacker, Molecular Transport Effects of Hydrocarbon Addition on Turbulent Hydrogen Flame Propagation, 2nd International Conference on Hydrogen Safety, EU NoE HySafe, San Sebastian, ES, 2007.

[36]. B. Johannessen. Studies of Combustion in Berkeley's Vitiated Co-flow Burner (VCB), Master's Thesis No. EPT-M-2011-16, Norwegian University of Science and Technology, 2011.

[37]. Y. Wu, Y. Lu, I.S. Al-Rahbi, G.T. Kalghatgi, Int. J. Hydrogen Energy 34 (14) (2009) 5940–5945.

[38]. R.S. Brokaw, Viscosity of Gas Mixtures. NASA Technical Note, NASA TN D-4496 (1968)

[39]. Montgomery, C.J., Kaplan, C.R. Oran, E.S. Proc. Combust. Inst. 27 (1998) 1175–1182.

[40]. N. Peters, J. Fluid Mech. 384 (1999) 107-132.

[41]. G.Z. Damköhler, Electrochem. 46 (1940) 601–626.

[42]. G.R. Ruetsch, L. Vervisch, A. Linan, Phys. Fluids 7 (1995) 1447–1454.

[43]. G.T. Kalghatgi, Combust. Sci. Technol. 26 (1981) 233–239.

[44]. A.D. Birch, D.R. Brown, M.G. Dodson, J. Fluid Mech. 88 (1978) 431–449.

[45]. W.M. Pitts, Combust. Flame 76 (1989) 197–212.